Journal of Zhejiang University-SCIENCE A

Flow structure and mixing characteristics of a transverse jet in supersonic crossflow under varied boundary layers

Cite this as: Yanhui ZHAO, Zhenfeng WANG, Shunping ZHANG, Shimao WANG, Xuechen LI, Ye TIAN, 2026. Flow structure and mixing characteristics of a transverse jet in supersonic crossflow under varied boundary layers. *Journal of Zhejiang University-SCIENCE A*, 27(9):1028-1042. https://doi.org/10.1631/jzus.A2500490

Wind tunnel facility & Optical diagnostics system

Mainstream flow experimental parameters

Experimental parameter	Value
Mainstream total temperature, T_0 (K)	300
Mainstream static temperature, T_∞ (K)	123.1
Mainstream total pressure, P_0 (Pa)	101325
Mainstream static pressure, P_∞ (Pa)	4488
Mainstream velocity, U_∞ (m/s)	596
Mainstream Mach number, Ma_∞	2.68
Unit Reynolds number, Re_u	9.068×10^6

Experimental injection parameters

Injection parameter	Value
Jet orifice diameter, d (mm)	2
Mach number, Ma_j	1
Total temperature, T_{0j} (K)	300
Total pressure, P_{0j} (kPa)	100, 300, and 500
Jet to mainstream dynamic pressure ratio, J	J_1=1.64, J_2=4.92, and J_3=8.19

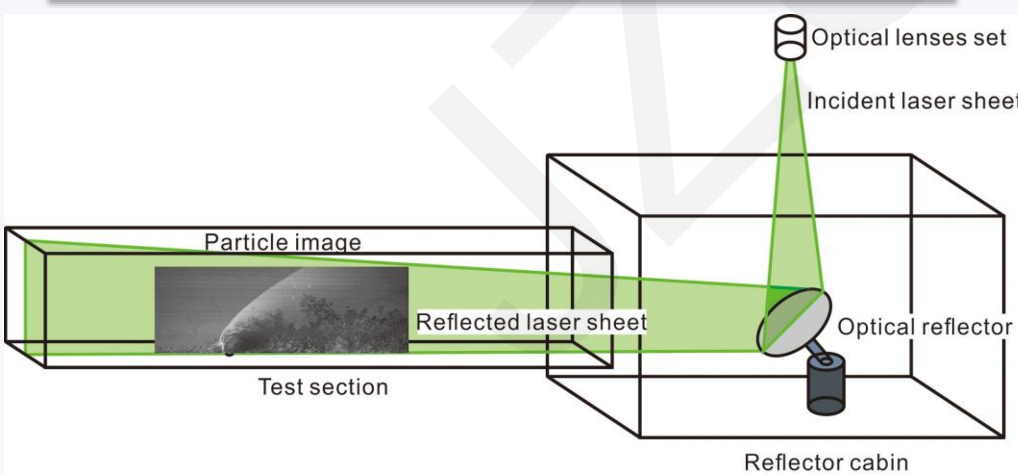

Observation sketch utilizing a reflector cabin

Direct-connect supersonic wind tunnel with reflector cabin

Mitigates wall reflection artifacts

Test section

120 mm x 56 mm rectangular cross-section

Field of view

394 mm (L) x 90 mm (H) optical access

Rayleigh/Mie Scattering

- Dual-cavity Nd:YAG laser (532 nm)
- TiO_2 nanoparticles (50 nm) / microparticles (0.5 um)
- CCD cameras: 4000x2672 pixel, 12-bit
- Temporal resolution: 10 ns
- Laser sheet thickness >= 0.5 mm

Stereoscopic PIV

- Two CCD cameras (Scheimpflug mounts)
- Interpulse interval: 0.5 us
- Least-squares 3D displacement
- Pin-hole model calibration (24x24)

Transient flow field topology & Velocity distribution

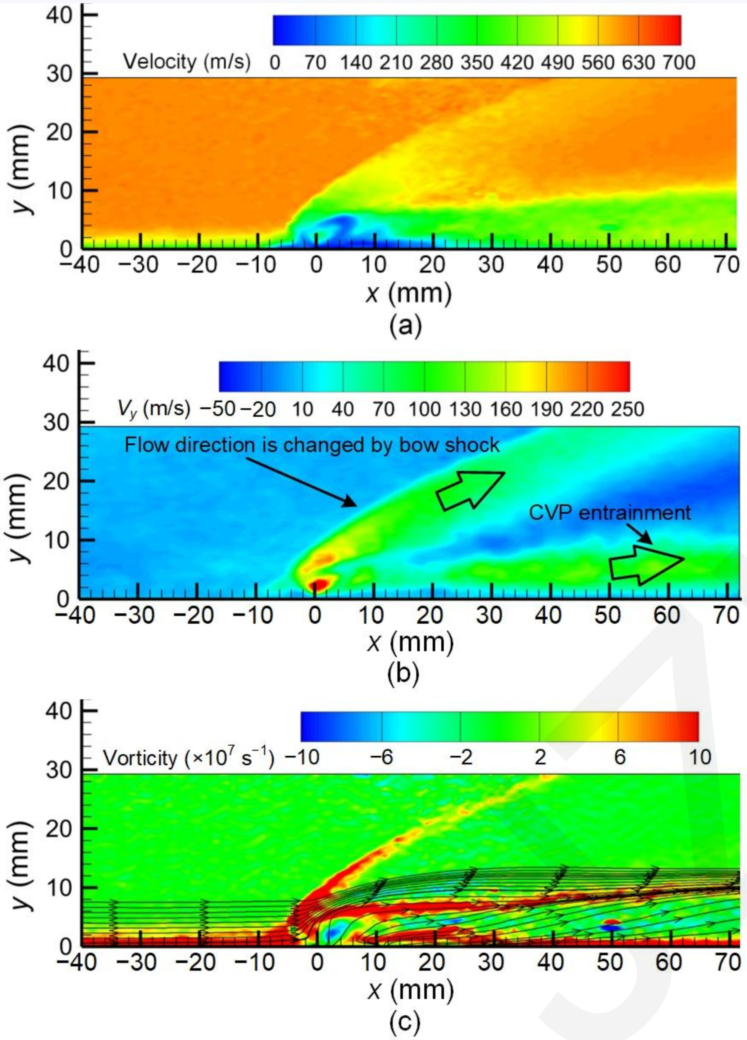

Fields of average velocity and vorticity for the XOY0 slice: (a) mean scalar velocity; (b) average y-axis velocity component; (c) mean vorticity field

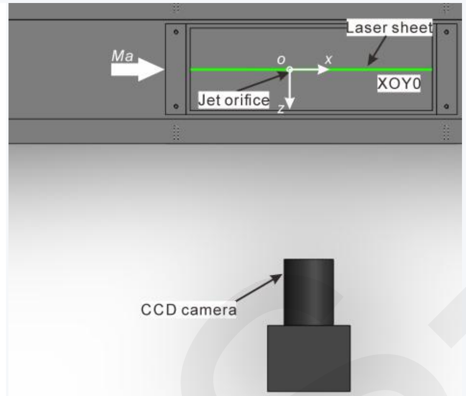

Arrangement of XOY slice observation

Barrel shock Length

~8 mm from orifice

Recirculation zone

~20 mm on leeward side

Mach disk length

~ Jet orifice diameter

Vertical velocity (V_y)

Pronounced jet uplifting momentum

Jet shear layer

Large-scale eddies roll up along the windward shear layer, with intense vorticity concentration driven by Kelvin–Helmholtz instabilities.

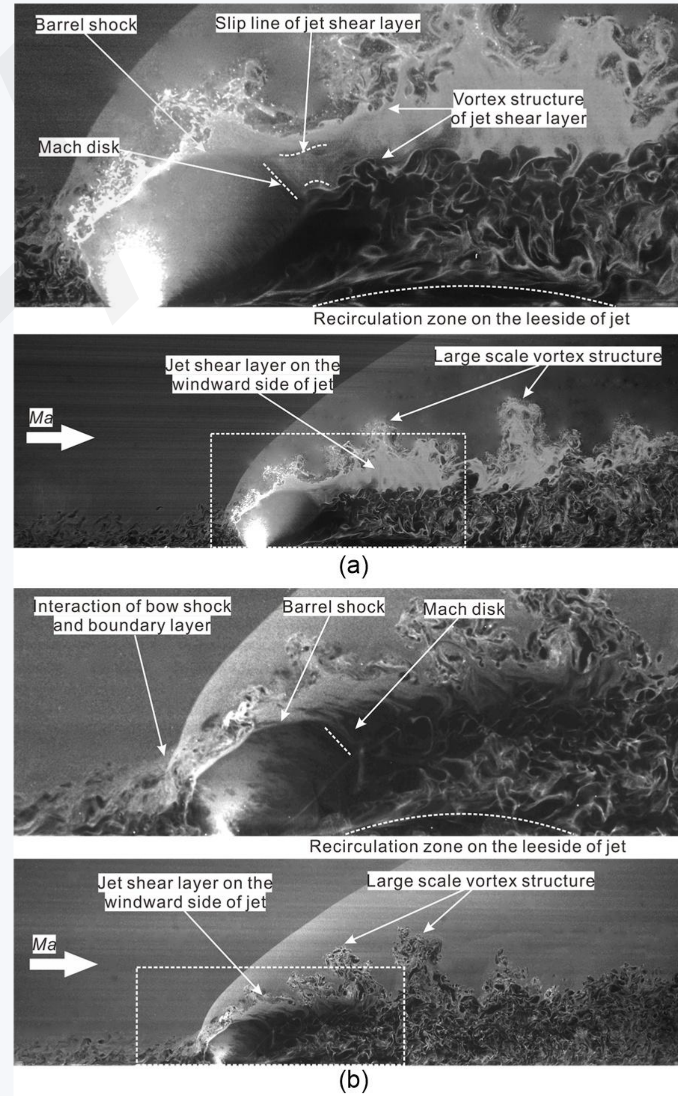

Gray images of the XOY0 slice in comparative experiments: (a) jet flow with particles; (b) jet flow without particles

Jet vortex system evolution: gray image sequence

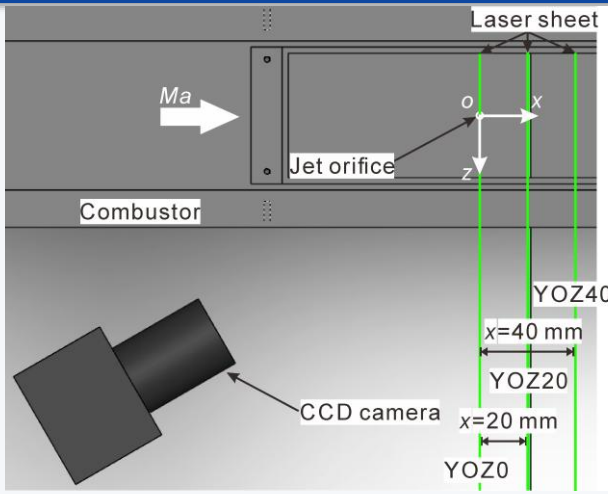

Location of YOZ slices

(a) A fan-shaped barrel shock forms at the jet exit;

(b) The counter-rotating vortex pair (CVP) rolls up on both sides of the jet plume;

(c) Coherent vortical structures emerge as the barrel shock weakens;

(d) Vortex cores of the prominent CVP become identifiable;

(e) Large-scale structures of the jet plume undergo significant breakup;

(f) The jet plume transitions into small-scale turbulent structures with significant vertical uplift

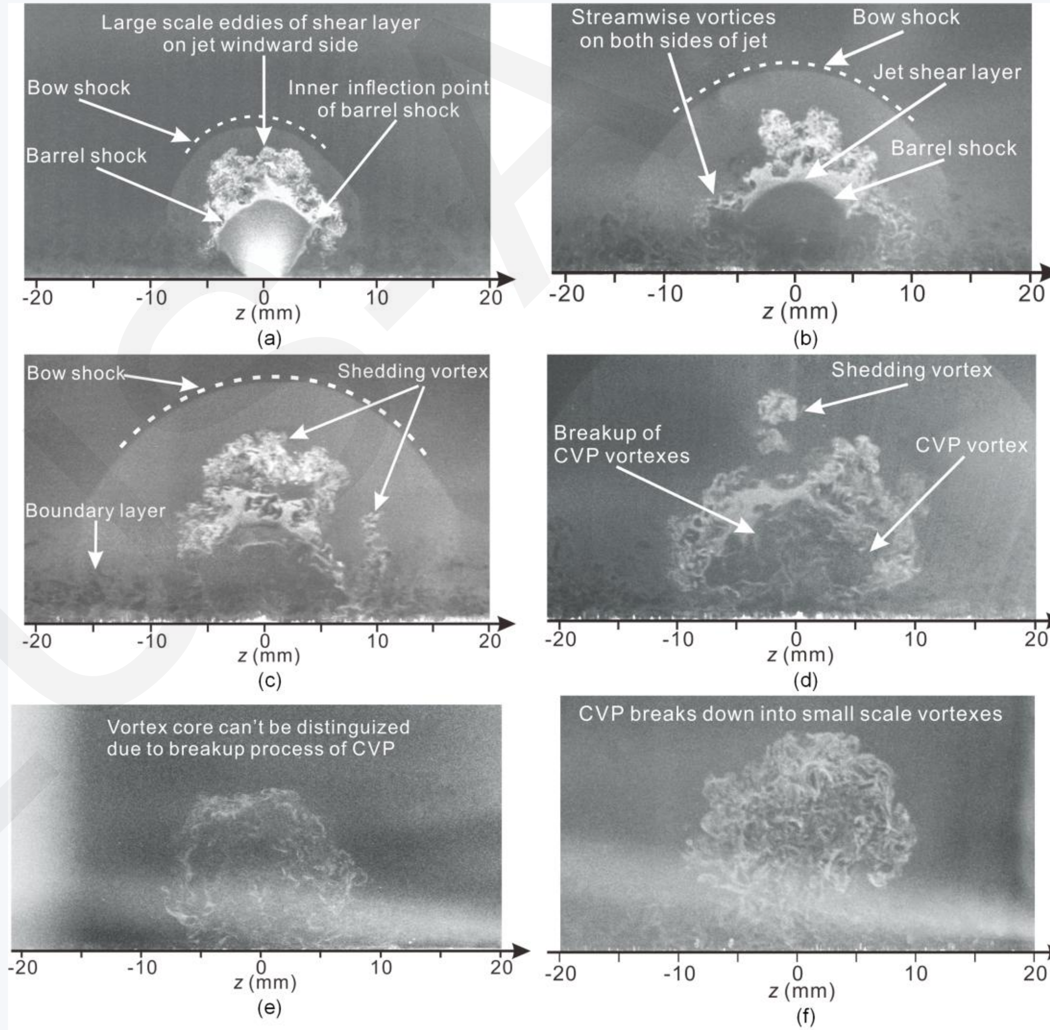

Instantaneous grayscale images of YOZ slices in the transverse jet flow field: (a) YOZ0; (b) YOZ5; (c) YOZ10; (d) YOZ20; (e) YOZ40; (f) YOZ100

Jet vortex system evolution: vorticity distribution maps

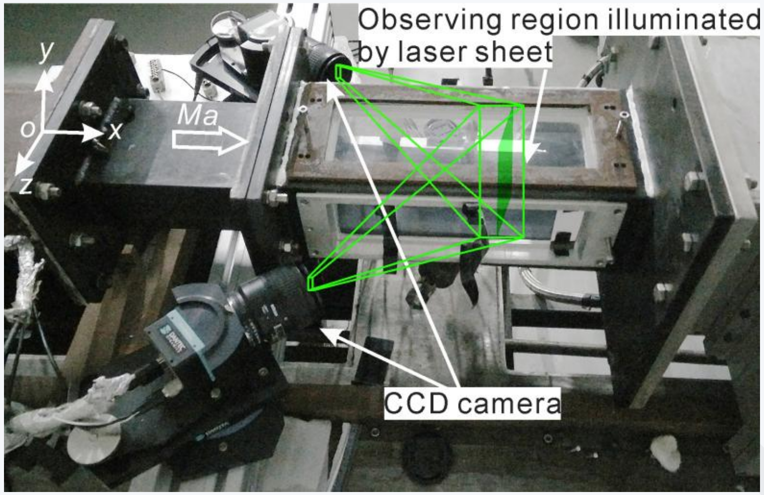

Two synchronized CCD cameras were set up on both sides of experimental model for velocity reconstruction.

Incipient Genesis: (a) YOZ0

At the jet exit, the CVP initiates as shear-layer vorticity begins to roll up, marking the onset of coherent vortex formation.

Entrainment & Growth: (b) YOZ10 and (c) YOZ20

In the near-field mixing region, streamwise vortices rapidly entrain ambient fluid into the plume. A fully established CVP emerges with strong counter-rotating cores, while induced secondary vortices of opposite vorticity develop beneath.

Reshape: (d) YOZ40, (e) YOZ60, (f) YOZ80

Axial distortion and vertical stretching reshape the CVP into a characteristic kidney-shaped vortex pair, enhancing far-field mixing.

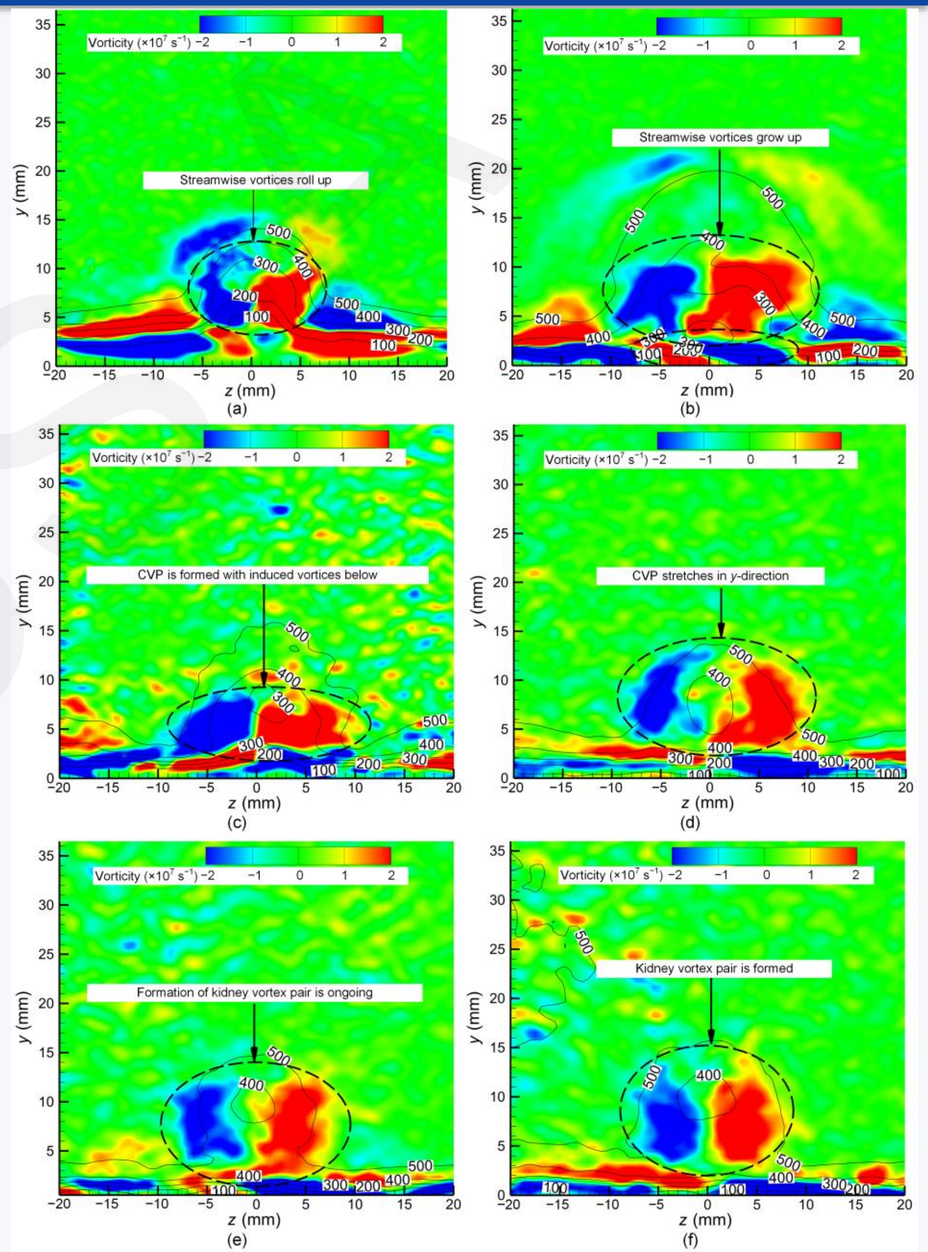

Penetration depth & Lateral diffusion

Penetration depth correlation expression:

$$\frac{P}{d} = AJ^{B}\left(\frac{x}{d}+C\right)^{E}\left(\frac{\delta}{d}\right)^{F}\left(\frac{Ma_j}{Ma_\infty}\right)^{G}$$

Study	Present study	Sun et al. (2013)
A	2.084	2.933
B	0.442	0.256
C	0	0
E	0.149	0.161
F	0.092	0
G	0	0

J: **the dynamic pressure ratio**
d: **jet orifice diameter**
x*/*d: **the dimensionless nozzle-to-orifice distance**
δ*/*d: **the dimensionless boundary layer thickness**
P*/*d: **the dimensionless penetration depth**

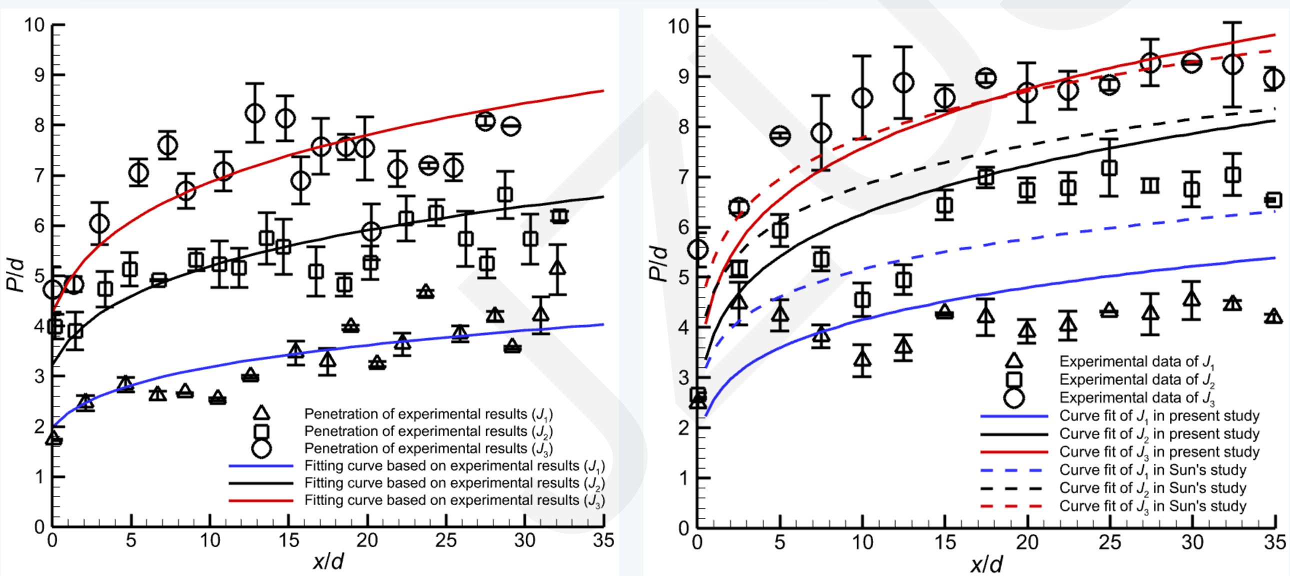

(a) **(b)**

Penetration depth variation of a transverse jet in supersonic crossflow for different boundary layer thicknesses: (a) 1 mm; (b) 4 mm

- **The present correlation demonstrates strong agreement with experimental data across all dynamic pressure ratios, whereas Sun et al.'s model overestimates penetration depths at low ratios.**
- **An increase in boundary layer thickness enhances the jet penetration depth in the far field by approximately 10%–20% across varying dynamic pressure ratios.**

Penetration depth & Lateral diffusion

Growth phases of lateral diffusion (δ=4mm, J=4.92)

Initial Stage: x=0~5d

At the jet orifice, lateral spreading peaks at approximately 7.5d (15 mm), driven by strong jet underexpansion and immediate radial pressure release.

Development Stage: x=5d~10d

From 5d to 10d, lateral diffusion expands rapidly to approximately 10d (20 mm). Streamwise vortex development enhances lateral mixing through entrainment amplification.

Stabilization Stage: x=10d~50d

Beyond x=10d, lateral diffusion stabilizes with negligible augmentation, as vorticity decay and kinetic energy dissipation eliminate driving mechanisms for further spreading.

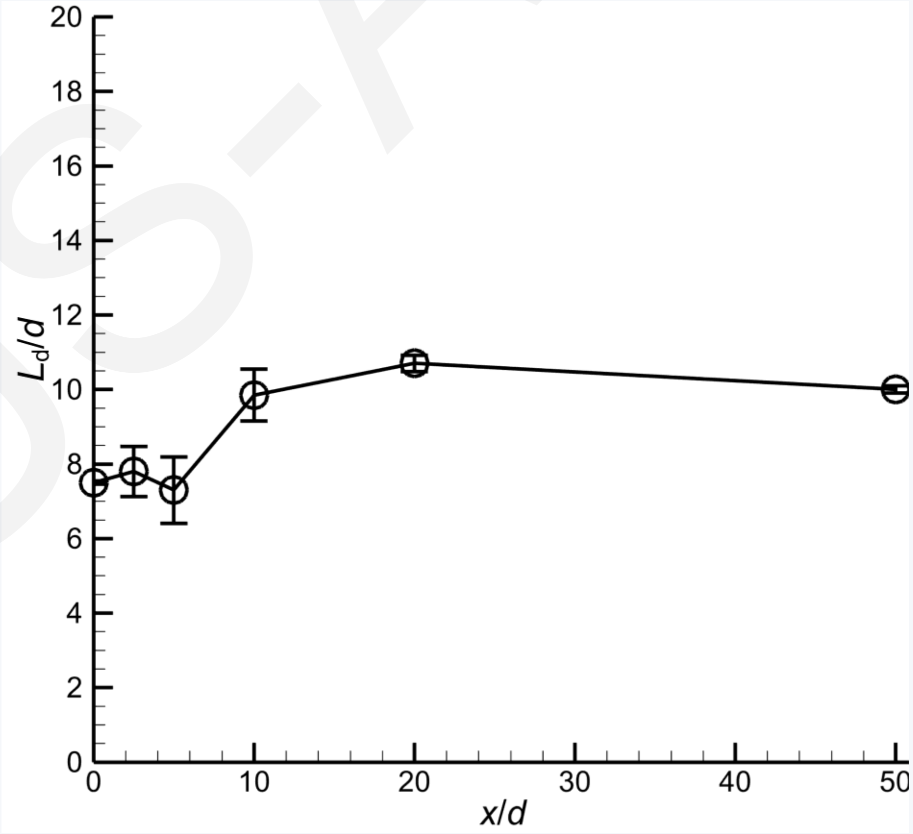

Lateral diffusion boundaries of the jet plume
(L_d/d is the dimensionless lateral diffusion boundary)

Fractal Dimension Analysis

Region I: Immediate Upstream

A sharp initial rise driven by shock–boundary layer interactions generating complex vortical structures. The fractal dimension is notably higher under the thick boundary layer (4 mm) than under the thin boundary layer (1 mm).

Region II: Near-Field Mixing Zone

Governed by competition between vortex merging (reducing complexity) and windward-side eddy generation (enhancing complexity), leading to variable trends across dynamic pressure ratios.

Region III: Far-Field Breakdown

Rapid, continuous increase peaking at approximately 1.6, driven by CVP development and subsequent breakup. The fractal dimension remains consistent across both boundary layer thicknesses (1 mm and 4 mm).

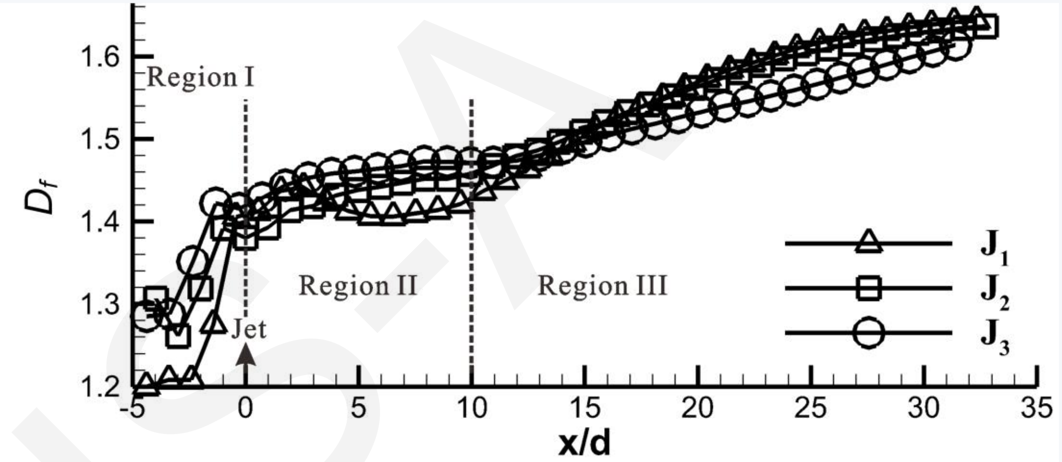

(a) 1mm

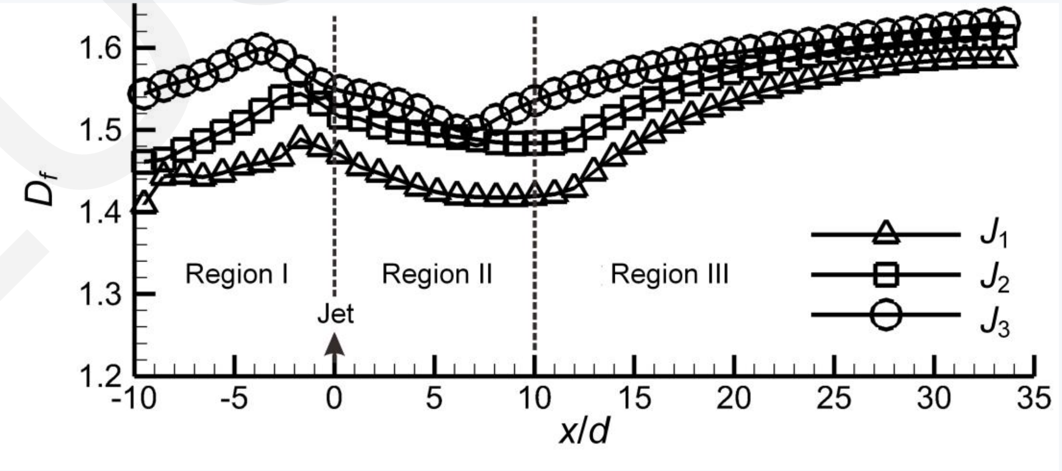

(b) 4mm

Streamwise distribution of the fractal dimension in the XOY0 slice for two boundary layer thicknesses